

The effect of pathologic venous valve on neighboring valves: fluid–structure interactions modeling

Elina Soifer¹ · Dar Weiss¹ · Gil Marom² · Shmuel Einav^{1,2}

Received: 24 May 2016 / Accepted: 15 September 2016 / Published online: 23 September 2016
© International Federation for Medical and Biological Engineering 2016

Abstract Understanding the hemodynamics surrounding the venous valve environment is of a great importance for prosthetic valves design. The present study aims to evaluate the effect of leaflets' stiffening process on the venous valve hemodynamics, valve's failure on the next proximal valve hemodynamics and valve's failure in a secondary daughter vein on the healthy valve hemodynamics in the main vein when both of these valves are distal to a venous junction. Fully coupled, two-way fluid–structure interaction computational models were developed and employed. The sinus pocket region experiences the lowest fluid shear stress, and the base region of the sinus side of the leaflet experiences the highest tissue stress. The leaflets' stiffening increases the tissue stress the valve is experiencing in a very low fluid shear region. A similar effect occurs with the proximal healthy valve as a consequence of the distal valve's failure and with the mother vein valve as a consequence of daughter vein valve's failure. Understanding the described mechanisms may be helpful for elucidating the venous valve stiffness–function relationship in nature, the reasons for a retrograde development of reflux and the relationship between venous valves located near venous junctions, and for designing better prosthetic valves and for improving their positioning.

Keywords Venous valve · Fluid–structure interaction · Computational model · Hemodynamics · Pathological valve

1 Introduction

Understanding the hemodynamics in the venous valve environment is of a great importance for the design of prosthetic valves. The leaflets of the venous valve are composed of collagen, elastin fibers and valvular interstitial cells, which have similar characteristics to smooth muscle cells. Thus, the leaflets respond to mechanical stimuli [7]. Stretching of these cells and fibers induce mechanotransduction, resulting in tissue remodeling. Pathological perturbations in the biomechanical environment of wall shear stress (WSS) and blood pressure can lead to various valvular diseases. These diseases are usually characterized with fibrosis induced by phlebitis, in which the leaflets' structure stiffens and the valve becomes more rigid.

Due to the level of complexity involved and the difficulty of achieving analytical solutions, different scenarios regarding the venous system are often analyzed using computer simulations. Buxton and Clarke [2] were the first to present a three-dimensional (3D) computational simulation focused on the dynamics of a venous valve. They captured the unidirectional nature of blood flow in venous valve and investigated the dynamics of the valve opening area and the blood flow rate through the valve. In this model, the vein was simulated as a rigid tube and the venous valve dimensions were not based on anatomical data. Furthermore, the applied pressure gradient was not physiological for veins [13, 15]. Zervides [17] reported on a 3D model of the venous valve which focused on the hemodynamics of the opening and closing phases. The results were used to develop a method of measuring blood 'washout' from behind the valve leaflets, and it was shown that gravity helps removing blood from the locations where flow stasis occurs [18]. However, the sinuses of the valve were not included even though they play an important role in

✉ Elina Soifer
elina_soifer@eng-alum.tau.ac.il

¹ The Department of Biomedical Engineering, Tel-Aviv University, Tel-Aviv, Israel

² Department of Biomedical Engineering, Stony Brook University, Stony Brook, NY, USA

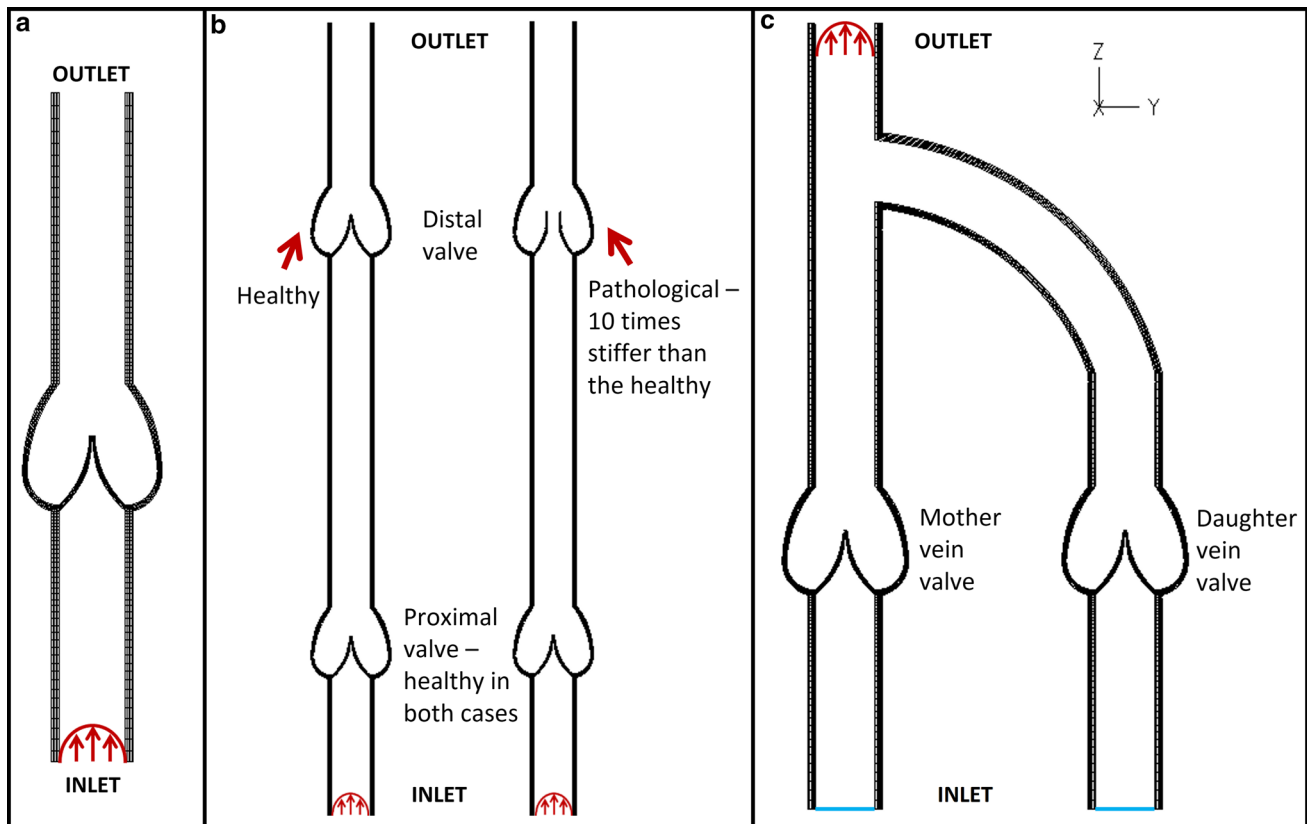


Fig. 1 Geometries of the **a** single venous valve model, **b** normal and abnormal cases in the model of two sequential venous valves, **c** model of two parallel venous valves

the local fluid dynamics [16]. Recently, Chen et al. [3] presented a biomechanical comparison between mono-, bi- and tricuspid venous valve architectures and the implications of such prosthetic designs on the flow and structure mechanics of the valves. They found that the mechanical cost, which was defined as the ratio between the internal structural stress and fluid wall shear stress (WSS) on the leaflets, was lowest for the bicuspid valve. However, the valves dimensions were not described and the designs did not include the sinuses of the bi- and tricuspid valves.

Although pathologically stiffer valves can affect their biomechanical condition and valve's failure can affect hemodynamics of their neighboring healthy valves, none of these studies investigated these phenomena. The aims of the present study are to evaluate the effect of (1) leaflets' stiffening process on the hemodynamics of the venous valve, (2) valve's failure on the hemodynamics of the next proximal valve and (3) valve's failure in a secondary daughter vein distal to a venous junction, on the hemodynamics of a healthy valve in the main vein distal to the junction. Fully coupled, two-way fluid–structure interaction (FSI) models were developed to model these scenarios.

2 Methods

2.1 Model of a venous valve: healthy versus pathological

A two-dimensional (2D) computational model of a typical venous valve geometry was constructed and studied. The vein was modeled with diameter of 4.3 mm and wall thickness of 0.5 mm [2], which are characteristic dimensions of the most proximal end of the greater saphenous vein [14]. The length of the domain was 4 cm (Fig. 1a).

The blood was assumed to be Newtonian fluid with density of 1060 kg/m^3 [4] and viscosity of 0.0035 Pa s [6]. To improve the convergence of the FSI model, the blood was assumed to be slightly compressible with a bulk modulus of 2.7 GPa [11]. The tissue was assumed to be isotropic, because it is a 2D model, and linear elastic with Poisson's ratio of 0.45 and Young's modulus of 1 and 0.2 MPa for vein wall [1] and 'healthy' valve leaflets, respectively. The elastic modulus of the healthy leaflets was adapted to allow a physiological opening of the valve, according to Lurie et al. [10]. Abnormal cases of fibrotic leaflets were modeled

by increasing the leaflets' elastic modulus, ranging between 200 and 1000 % larger than the healthy reference state.

A laminar parabolic flow profile with a maximal velocity of 7 cm/s was assigned to the model inlet [10], while a uniform fluid pressure of 0 Pa was set at the outlet as a reference for calculation of pressure differences across the valve. The wall was fixed near the inlet and outlet boundaries and was constrained to prevent lateral expansion. We assumed that the motion of the vein wall is defined mainly by the external pressure of the muscles and not by the blood flow, but the blood flow define the motion of the valve leaflets. Thus, the unknown motion of the vein wall was ignored, and an almost rigid wall behavior was used. Gravity body force was considered in Z-direction. The FSI interfaces were defined at the surfaces of the vessel wall, sinus and leaflets. Contact interaction was set up between the two leaflets, preventing penetrations between them. The axial velocity magnitudes proximal and distal to the valve and between its leaflets were examined.

The structural part was discretized with a mesh of 2000 plane strain elements, 550 of them comprised the leaflets. The flow domain was discretized with a mesh of approximately 10,000 planar elements. Time discretization of 0.5 ms was used. The fluid domain was governed by Navier–Stokes and continuity equations, while the solid domain was governed by the momentum and equilibrium equations. A fully coupled, two-way FSI analysis was implemented, using the commercial finite-element package ADINA (version 9.0, Watertown, NY, USA). The arbitrary Lagrange–Eulerian (ALE) method was also employed to allow the fluid mesh deform with the leaflets motion.

For evaluation of the valve's condition, leaflet's tissue stresses and fluid WSS were analyzed for the base region of the sinus side of the leaflets, as it is a critical area prone to valve pathology [3] and it is expected to develop the maximal tissue stress values. In addition, the pressure gradient across the valve, calculated as the difference between blood pressures proximal and distal to the valve (vertical distance of 7.6 mm), was examined.

Furthermore, cross-sectional area between the leaflets at the maximal opened state of the valve was compared with the cross-sectional area distal to the valve. Cross-sectional area calculations assumed that the effective cross-sectional area of the vein was circular above and below the valve and elliptic in a maximally open valve state, with the longer axis equal to the diameter of the sinus and the shorter axis equal to the distance between the leaflets [10].

2.2 Model of two sequential venous valves

The 2D geometry of a single venous valve was extended to a pair of sequential venous valves geometry (Fig. 1b).

The length of the domain was 8.5 cm, while the distance between the valves was 3.8 cm, which is the mean distance between paired valves in the Greater Saphenous Vein [9].

In this model, a limited elasticity was given to the vein wall to prevent the mass conservation from dictating identical flow rate through both valves and to allow capturing the phase difference between them. Vein wall was modeled with a Young's modulus of 10 GPa, assuming that it is almost rigid, as in the previous case. Due to the static pressure resulting from the segment length, the elastic modulus of the healthy valve was increased from the previous section to 1 MPa, while still being in the physiological range [12]. The boundary conditions remained unchanged. The wall was fixed near the inlet and the outlet boundaries.

The pathology of the distal fibrotic valve was modeled by increasing its leaflets' elastic modulus 10 times higher than in the healthy proximal valve. Furthermore, the pathological valve remained open throughout the simulation to model a non-functional valve which can no longer prevent a retrograde flow, while its leaflets remained suspended in the flowing stream. For evaluation of the proximal (healthy) valve's condition, for both healthy and pathological distal valves, this valve was analyzed as described in Sect. 2.1.

2.3 Model of two parallel venous valves (venous junction)

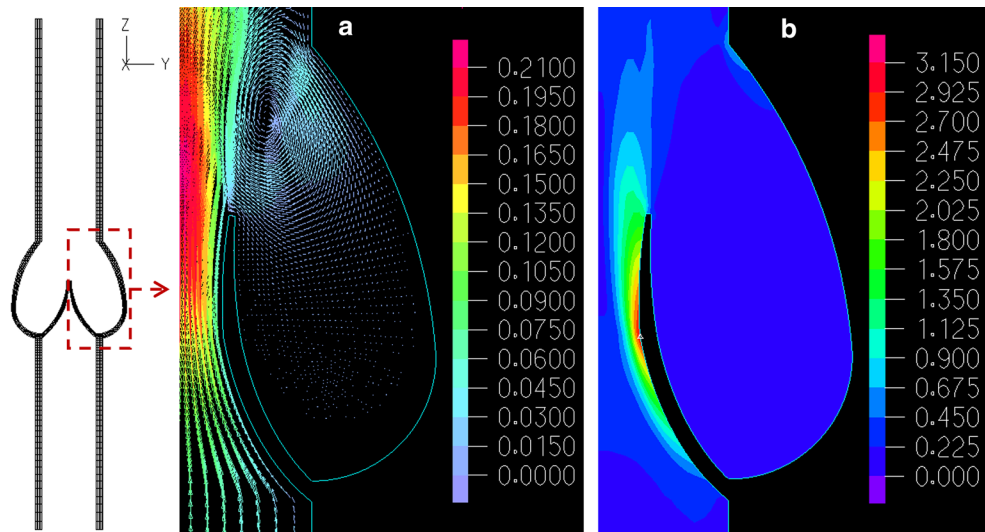
The 2D single venous valve geometry was extended to geometry of two parallel venous valves, associated with a venous junction shape (Fig. 1c). The length of the domain was 5.5 cm.

The material properties used for the vein wall and healthy valve leaflets were as described in Sect. 2.1. Similar to previous case, pathological case in which the daughter vein's valve (right valve) is fibrotic was modeled by increasing this valve's elastic modulus by 10 times.

A spatially uniform fluid pressure was assigned at the model inlets, while a parabolic spatial flow function with a maximal velocity of 10 cm/s was set at the outlet [10]. These boundary conditions were necessary to examine the influence of one valve on the other because velocity inlet boundary conditions would have dictate flow rates through each valve. The unknown motion of the vein wall was ignored and an almost rigid wall behavior was used, as described in Sect. 2.1.

The left (healthy) valve's condition was evaluated for healthy and pathological right valve, analyzing its leaflet's tissue stress at the base region of the sinus side of the leaflet and the pressure gradient it was subjected to.

Fig. 2 **a** Vector flow field for the healthy valve (m/s). **b** Fluid WSS distribution for the healthy valve (Pa)



3 Results

3.1 Mesh and time step refinement studies

The FSI simulation described in Sect. 2.1 has been employed to test the meshes of the flow and structural domains. A coarse mesh with approximately 10,000 flow elements and 550 structural leaflet elements was compared with a fine mesh with approximately 20,000 flow elements and 1100 structural leaflet elements. Time-averaged relative errors for the leaflet's tissue stress in the base region of the leaflet's sinus side, the lateral displacement of the leaflet's free edge, the flow axial velocity between the leaflets' free edges and the pressure gradient on the valve were smaller than 6 % (5.87, 2.77, 3.95 and 0.91 %, respectively). Consequently, the coarse mesh was employed in the single-valve model (Sect. 2.1) and was correspondingly extended in the following models (Sects. 2.2, 2.3).

Time discretization quality was tested using the same model with time steps of 0.5 and 0.25 ms. Time-averaged relative errors were calculated for the same parameters described above and were below 1.5 % (0.72, 1.48, 1.06 and 0.93 %, respectively). Consequently, a time step of 0.5 ms was used for all models.

3.2 Comparison of healthy and pathological venous valves

The flow field and the fluid shear stress for the healthy valve are shown in Fig. 2. A stagnation region of low fluid velocity and WSS can be identified behind the leaflets in the sinus pockets. In all four cases of valve elasticity, a jet was formed between the upper parts of the leaflets, the narrowest region for the flow. Figure 3 depicts the effective

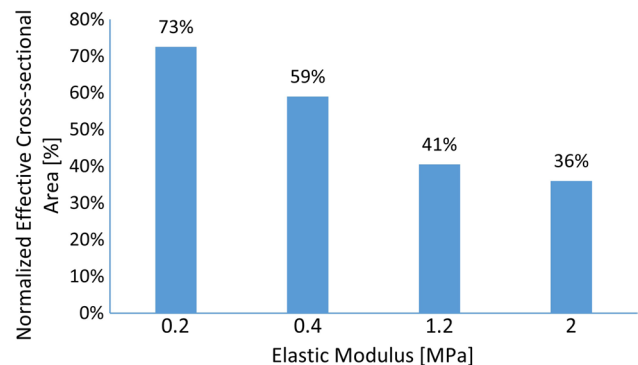


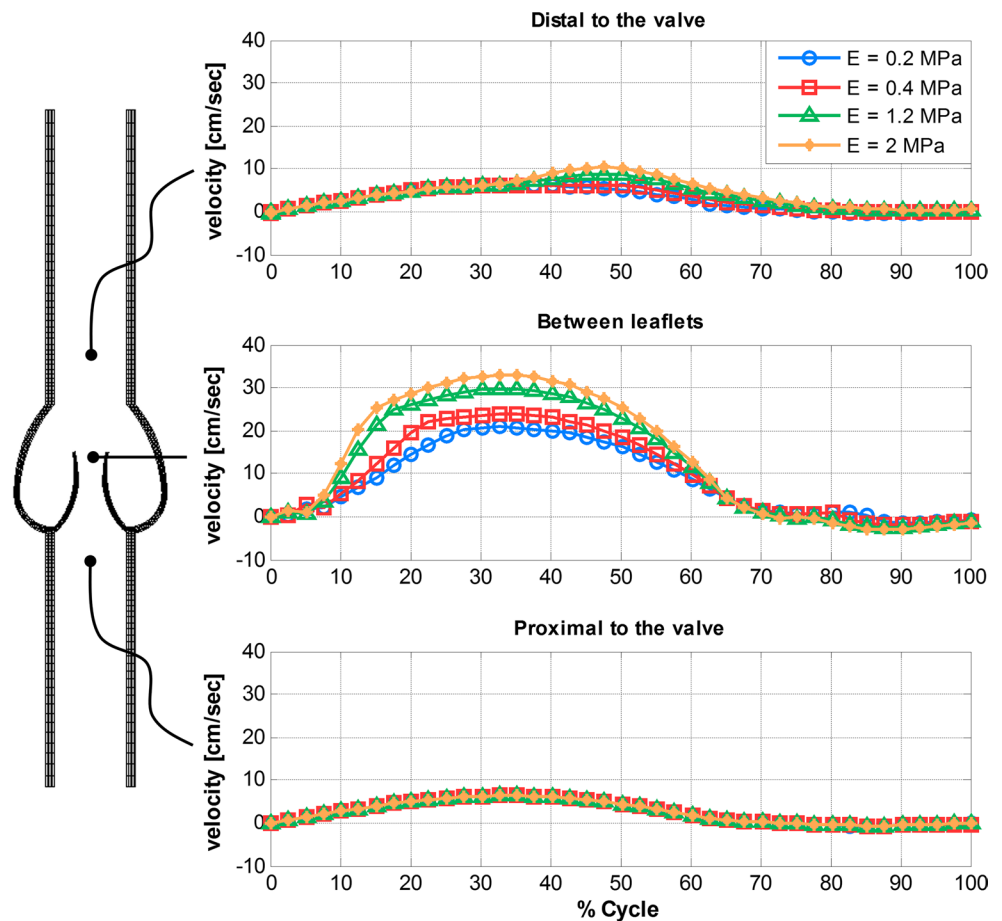
Fig. 3 Normalized effective cross-sectional area between the leaflets in a maximally open valve state as a percent of the cross-sectional area distal to the valve for each of the tested elastic moduli

cross-sectional area between the leaflets in a maximally open valve state as a percent of the cross-sectional area distal to the valve for each of the tested elasticity moduli. As the leaflets stiffen their range of motion becomes smaller. As a result, the cross-sectional area between the leaflets decreases and that causes a stronger jet, as shown in Fig. 4.

Figure 5 depicts the dynamics of the leaflet tissue stress at the base region of the sinus side of the leaflet and the dynamics of the pressure gradient on the valve, for the four cases with various stiffnesses. It can be noticed that the leaflet tissue stress increases with the increase in the leaflet's stiffness. It can be also noticed that the blood pressure difference across the valve, especially in the closed phase, increases with the leaflet's stiffening.

The tissue stress for the healthy valve is shown in Fig. 6. As expected, the maximal tissue stress is developed at the base region of the sinus side of the leaflet. The sinus pocket region experiences the lowest fluid shear (Fig. 2), and the

Fig. 4 Waveforms of the axial velocity distal to, between the leaflets of, and proximal to the healthy valve



base of the leaflet experiences the highest tissue stress value. Thus, this region is vulnerable for thrombosis and hyperplasia.

3.3 The influence of pathologic valve on the next proximal valve

Figure 7 depicts the dynamics of the leaflet tissue stress at the base region of the sinus side of the leaflet, and the dynamics of the pressure gradient across the valve, for the healthy valve in both cases. The maximal leaflet tissue stress in the abnormal case is 73 % greater than in the normal case. It can be noticed that the pressure gradient that the healthy valve is subjected to in the abnormal case, during the closed phase, is much larger than in the normal case. The maximal pressure gradient in the abnormal case reaches 316 % of the maximal pressure gradient in the normal case.

The effective cross-sectional area between the healthy valve’s leaflets in a maximally open valve state, as a percent of the cross-sectional area distal to the valve, was 54 and 45 % in the normal and abnormal cases, respectively. Therefore, there was a decrease of about 16 % in the maximal effective cross-sectional area in the abnormal case compared with the normal case.

3.4 The influence of pathologic valve on parallel valve in the mother vein

Figure 8 depicts the dynamics of the leaflet tissue stress at the base region of the sinus side of the leaflet, and the dynamics of the pressure gradient on the valve, for the left (healthy) valve in both cases. The maximal leaflet tissue stress in the abnormal case is 380 % of the maximal leaflet tissue stress in the normal case. It can be noticed that the blood pressure difference which the left valve is subjected to in the abnormal case, during the closed phase, is much larger than in the normal case. The maximal pressure difference in the abnormal case is 353 % of the normal case.

4 Discussion

This study presents 2D FSI numerical models of realistic typical venous valves and is the first to model and examine pathological venous valves. Previous models of venous valves either used a geometry that was not based on anatomical data [2] or were not physiologically correct since the sinuses of the valve were not considered [3, 17]. The present model’s geometry is based on anatomical data and includes

Fig. 5 **a** Dynamics of leaflet tissue stress for the four valves with various stiffnesses at the base region of the sinus side of the leaflet. **b** Dynamics of the pressure gradient across the valve

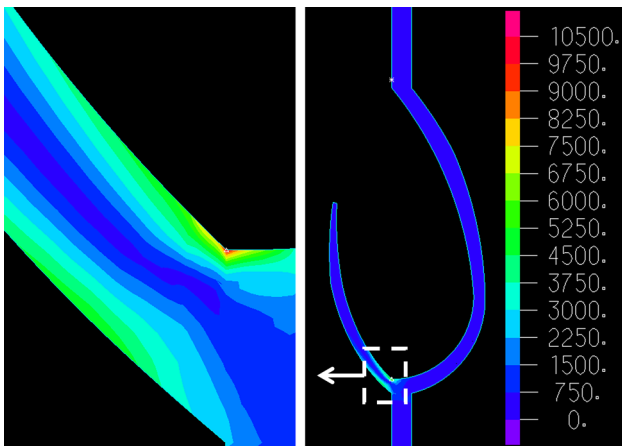
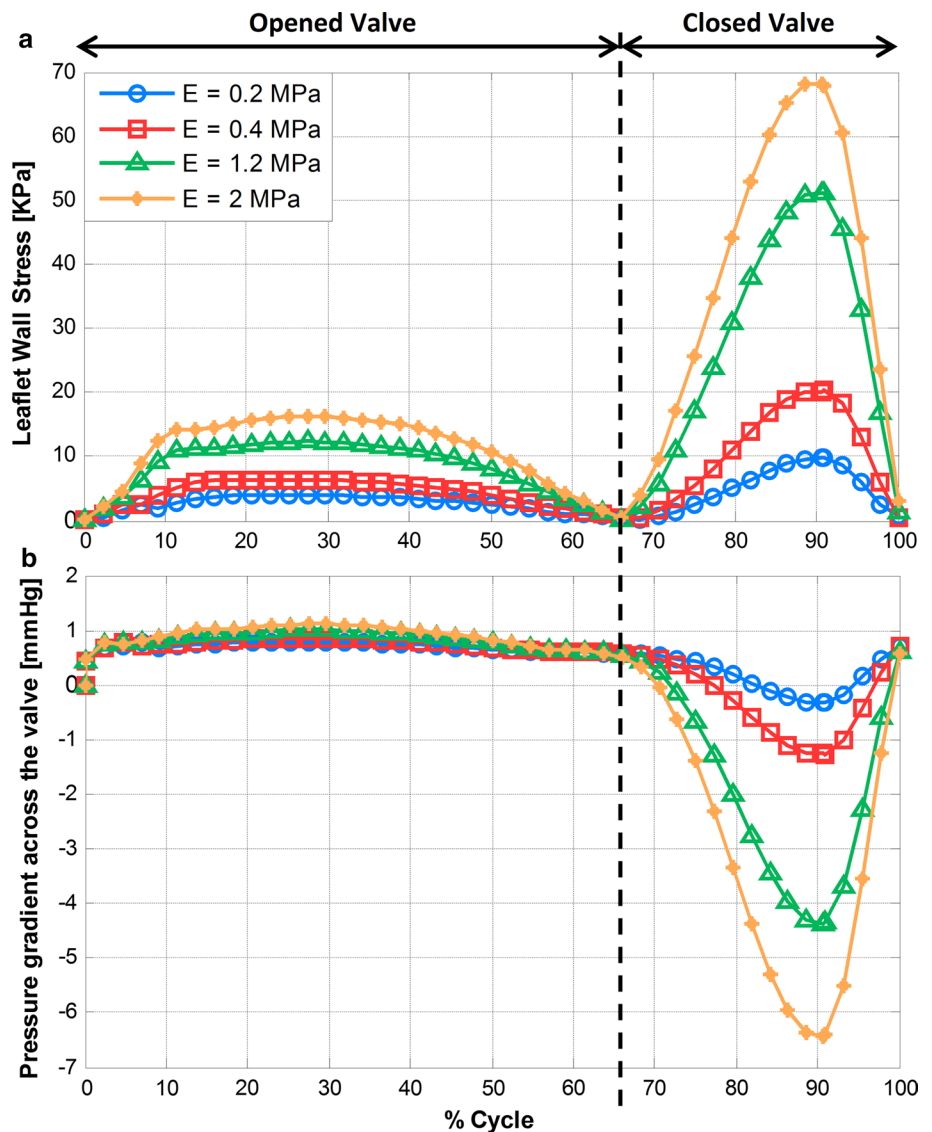
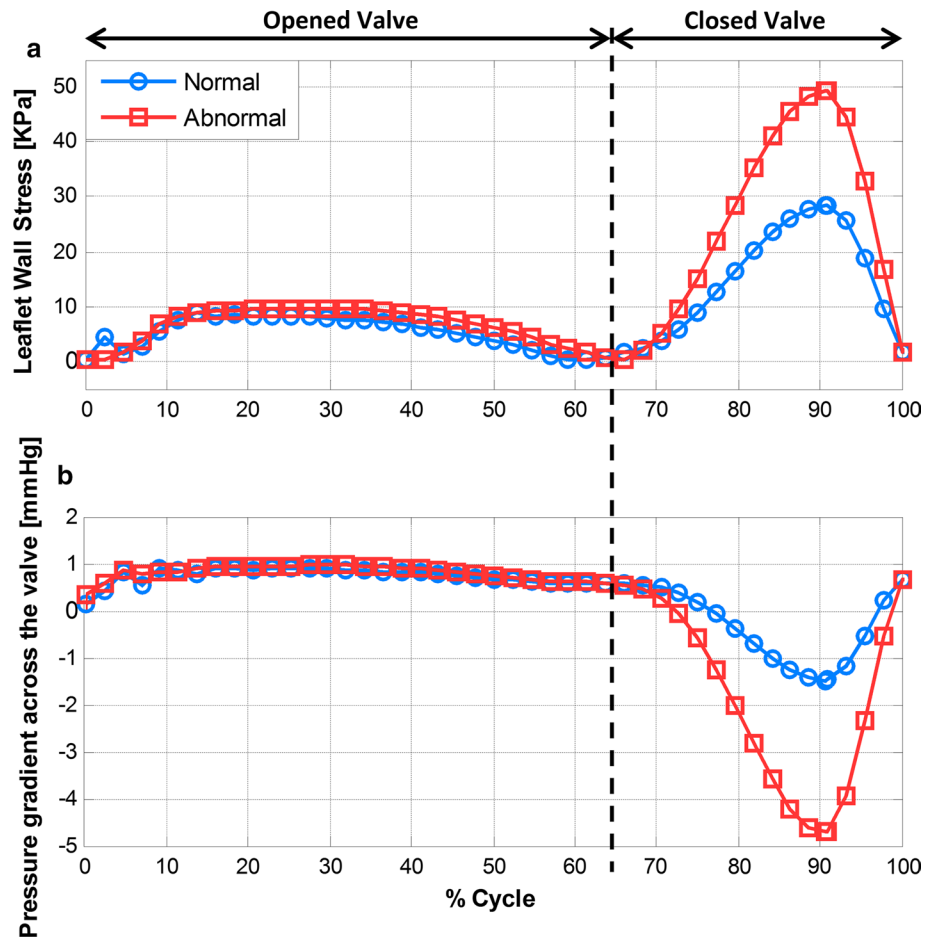


Fig. 6 Tissue stress for the healthy valve (Pa) with zoom into the base of the leaflet region

the sinuses of the valve. The existence of the sinuses in the current model allows examination of the most sensitive region of the leaflet in terms of tissue stress (Fig. 6) and of the sinus pocket area, which is prone to valve pathology. Furthermore, the current model employs realistic and physiological pressure and flow boundary conditions, unlike previous attempts to model venous valves [2].

The current 2D model represents the symmetric cross section of a 3D geometry. This cross section is equivalent to an ultrasound view during evaluation of venous valve performance. Although the examined parameters in this study would probably differ in their magnitude from 3D model results, the dynamics would be very similar. The main advantage of a 2D model is that it requires significantly less elements and degrees of freedom, which lead to significantly faster solution time with lower required computing power. The typical solution time on our available hardware

Fig. 7 Comparison of both cases of the sequential venous valves geometry. **a** The dynamics of leaflet tissue stress for the healthy valve at the base region of the sinus side of the leaflet. **b** The dynamics of the pressure gradient for the healthy valve



was about 2 h for the models with two valves. Similar ALE models with dynamic meshes but in 3D, could take weeks to solve, because they require extremely fine mesh.

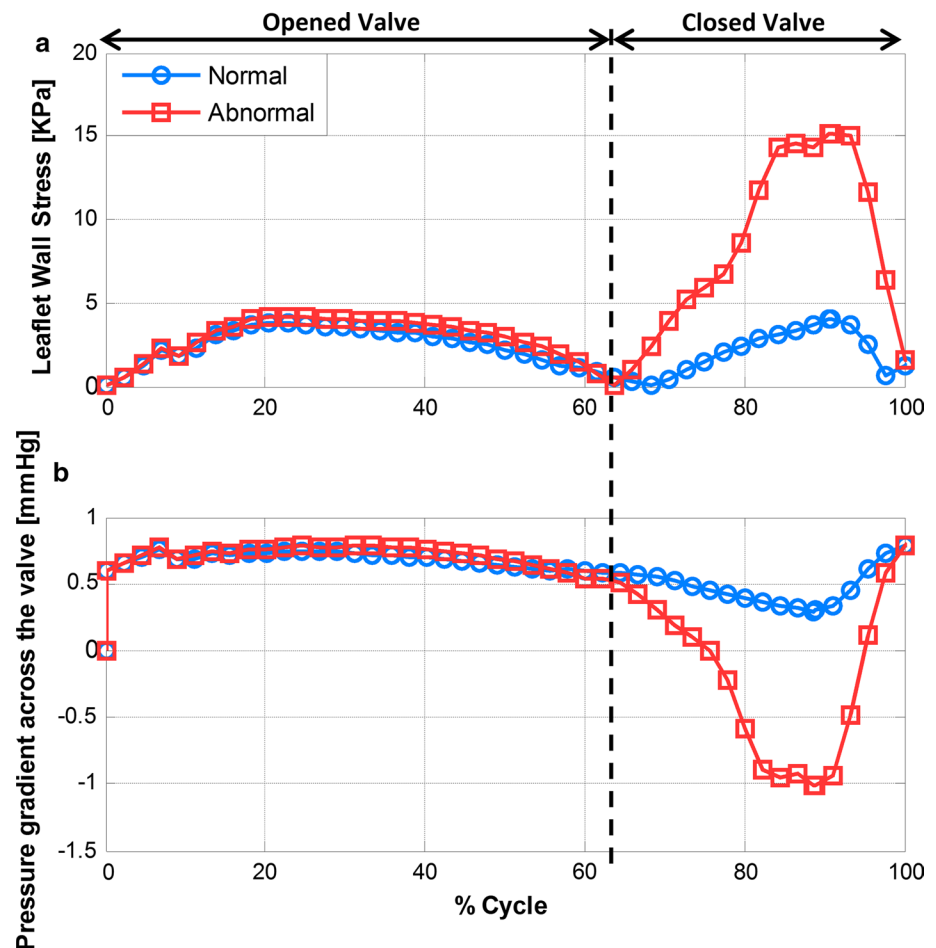
All the models of the present study showed that the sinus pocket region experiences the lowest fluid shear stress and the base region of the sinus side of the leaflet experiences the highest tissue stress. Fluid WSS is known to be sensed by the endothelium and to initiate mechanotransduction [3]. Regions with relative stagnation, such as the valve’s sinus pockets, are prone to phlebitis because of increased adhesion of thrombotic and inflammatory cells. Structural stresses affect the cells and fibers within the wall and induce mechanotransduction, biological and pathological responses [3]. Higher fluid shear stress in the sinus pocket and lower tissue stress in the leaflets are more favorable.

Valve failure in the venous system may be secondary to phlebitis [5] which leads to valve rigidity. Rigid valve leaflets are characterized with increased collagen content and reduced elastin content. As a consequence, the valve becomes fibrotic and its elasticity is damaged. The current model with varying elasticity demonstrate that as the valve leaflets stiffen, the leaflets tissue stress at the sinus side of its base region increases, and as the valve is subjected to

higher blood pressure gradient, the leaflet’s range of motion is decreased, and a stronger jet is formed between the leaflets’ free edges. These phenomena may lead to a worse biomechanical condition of the valve, higher tissue stress in a very low fluid shear region. It suggests that the valve is vulnerable to phlebitis and that this process activates itself until the valve is totally damaged. Understanding the described mechanism may be helpful for elucidating the venous valve stiffness–function relationship in nature and for designing better prosthetic valves.

This study also presents the first computational model of two sequential venous valves and the interaction between them. A case of two normal valves was compared to a case in which the distal valve is non-functional. This comparison demonstrates the effect of valve’s failure on the biomechanical condition of the next proximal valve. It was shown that the failure of the distal valve causes the proximal healthy valve to experience higher stress on its leaflets since the pressure gradient that the healthy valve is subjected to increases significantly. In addition, the effective cross-sectional area between the healthy valve leaflets in a maximally open valve state decreases, which indicates that its leaflets’ range of motion is reduced. It illustrates that

Fig. 8 Comparison of both cases of the venous junction geometry. **a** The dynamics of leaflet tissue stress for the healthy valve at the base region of the sinus side of the leaflet. **b** The dynamics of the pressure gradient for the healthy valve



the biomechanical condition of the proximal healthy valve becomes hemodynamically less favorable as a consequence of the distal valve's failure. Understanding the described mechanism is helpful for elucidating the reasons for a retrograde development of reflux [8].

Furthermore, this study presents the first computational model of two parallel venous valves, associated with a venous junction. A case of two normal valves was compared with a case in which the daughter vein's valve was pathological, in order to examine the effect of valve's failure in the daughter vein on the biomechanical condition of the valve in the mother vein, both valves near the junction. It was shown that the stiffening of the daughter (right) vein's valve caused the left healthy valve to experience higher stress in its leaflets. It can probably be explained by the blood pressure difference that the left valve is subjected to is significantly higher than in the healthy case. This indicates that the biomechanical condition of the mother vein valve became less favorable as a consequence of daughter vein valve's failure. Understanding the described mechanism may be helpful for elucidating the relationship between venous valves located near venous junctions and for improved positioning of prosthetic valves.

5 Conclusions

The described realistic models allow estimating how pathological stiffening of the valve leaflets changes the valve biomechanical condition, and the effect of pathological venous valves on neighboring valves in two different constellations. These models may be helpful for elucidating the venous valve stiffness–function relationship in nature, the reasons for a retrograde development of reflux and the relationship between venous valves located near venous junctions, for designing efficient prosthetic valves and for improving their positioning. Future studies might employ 3D models of neighboring valves in sequence to find the influence of their relative angle on the hemodynamics and the flow pattern.

References

1. Buescher C, Nachiappan B, Brumbaugh J, Hoo K, Janssen H (2005) Experimental studies of the effects of abnormal venous valves on fluid flow. *Biotechnol Prog* 21:938–945
2. Buxton GA, Clarke N (2006) Computational plebology: the simulation of a vein valve. *J Biol Phys* 32:507–521

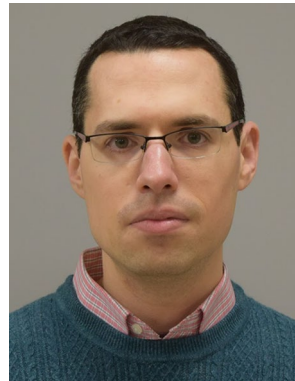
3. Chen HY, Berwick Z, Krieger J, Chambers S, Lurie F, Kassab GS (2014) Biomechanical comparison between mono-, bi-, and tricuspid valve architectures. *J Vasc Surg Venous Lymphat Disord* 2(188–193):e181
4. Cutnell J, Johnson K (1998) *Physics*, 4th edn. Wiley, New York
5. Eberhardt RT, Raffetto JD (2005) Chronic venous insufficiency. *Circulation* 111:2398–2409
6. Formaggia L, Veneziani A (2003) Reduced and multiscale models for the human cardiovascular system. *Lecture Notes VKI Lecture Series 7*
7. Huang H-YS, Liao J, Sacks MS (2007) In-situ deformation of the aortic valve interstitial cell nucleus under diastolic loading. *J Biomech Eng* 129:880–889
8. Labropoulos N, Giannoukas AD, Delis K, Mansour MA, Kang SS, Nicolaides AN, Lumley J, Baker WH (1997) Where does venous reflux start? *J Vasc Surg* 26:736–742
9. Lurie F, Kistner R (2012) The relative position of paired valves at venous junctions suggests their role in modulating three-dimensional flow pattern in veins. *Eur J Vasc Endovasc Surg* 44:337–340
10. Lurie F, Kistner RL, Eklof B, Kessler D (2003) Mechanism of venous valve closure and role of the valve in circulation: a new concept. *J Vasc Surg* 38:955–961
11. Marom G (2015) Numerical methods for fluid–structure interaction models of aortic valves. *Arch Comput Methods Eng* 22:595–620
12. Marom G, Haj-Ali R, Raanani E, Schäfers H-J, Rosenfeld M (2012) A fluid–structure interaction model of the aortic valve with coaptation and compliant aortic root. *Med Biol Eng Comput* 50:173–182
13. Meissner MH, Moneta G, Burnand K, Gloviczki P, Lohr JM, Lurie F, Mattos MA, McLafferty RB, Mozes G, Rutherford RB (2007) The hemodynamics and diagnosis of venous disease. *J Vasc Surg* 46:S4–S24
14. Spivack DE, Kelly P, Gaughan JP, van Bemmelen PS (2012) Mapping of superficial extremity veins: normal diameters and trends in a vascular patient-population. *Ultrasound Med Biol* 38:190–194
15. Thiriet M (2015) Physiology and Pathophysiology of Venous Flow. *PanVasc Med*. 569–589. doi:[10.1007/978-3-642-37078-6_27](https://doi.org/10.1007/978-3-642-37078-6_27)
16. Tien W-H, Chen H, Berwick Z, Krieger J, Chambers S, Dabiri D, Kassab G (2014) Role of sinus in prosthetic venous valve. *Eur J Vasc Endovasc Surg* 48:98–104
17. Zervides C (2010) 3D modelling of a venous valve: how effective are postural changes under gravity, in ‘washout’ recirculatory regions in the lee of venous valves? *Pliroforiki*:38–44
18. Zervides C, Giannoukas A (2013) Computational phlebology: reviewing computer models of the venous system. *Phlebology* 28:209–218



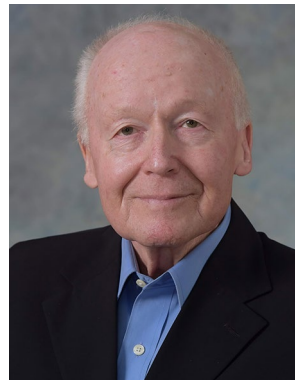
Elina Soifer received her M.Sc. degree in Biomedical Engineering from Tel-Aviv University. In her research, she studied the hemodynamics of venous valves, both healthy and pathological, using FSI 2D and 3D modeling.



Dar Weiss (M.Sc.) is a Ph.D. student at the Engineering Faculty, Tel-Aviv University. His research focus is biomechanical aspects of thrombophlebitis related catheters in peripherally located veins.



Dr. Gil Marom (Ph.D.) is a Postdoctoral Associate at Stony Brook University, NY, USA. He develops numerical methods for fluid–structural interaction modeling with a focus on cardiovascular valves.



Prof. Shmuel Einav is a Research Professor at Stony Brook University and an Emeritus Professor of Tel-Aviv University. His research interests are in Biofluid Mechanics, cardiovascular circulation, healthcare and medical devices.